Performance of LTE ADVANCED Uplink in a Flat Rayleigh Channel

Edward KASEM, Roman MARSALEK, Jiri BLUMENSTEIN

Department of Radio Electronics, Faculty of Electrical Engineering and Communications, Brno University of Technology, Technicka 12, 616 00 Brno, Czech Republic

xkasem01@stud.feec.vutbr.cz, marsaler@feec.vutbr.cz, xblume00@stud.feec.vutbr.cz

Abstract. *This paper describes the performance of LTE advanced uplink transmission in a flat Rayleigh channel. The uplink is simulated using a modified version of the Vienna uplink link level matlab code simulator. This modified version supports two transmission antennas instead of one. Moreover, it includes two extra processes; layer mapping and precoding. In addition, the demodulation reference signal is presented and employed to allow channel estimation. In this paper, the structure of the LTE advanced system is described. Furthermore, we present generation of the demodulation reference signal. Four combinations of two distinct channel estimation and two signal detection methods are used to provide the simulation results of performance evaluation in term of the BER and throughput curves for selected scenarios.*

Keywords

BER, Flat Rayleigh, LTE advanced, LS, MMSE, SSD, ZF.

1. Introduction

The 3rd Generation Partnership Project (3GPP) Long Term Evolution (LTE) Standard Release 10 [1], commonly named as Long Term Evolution Advanced (LTE-A), is the next major milestone in the evolution of LTE (Release 8).

This paper is a result of modifying the uplink link level matlab code simulator in order to support a new feature compared to LTE uplink link level simulator and fulfill LTE-A requirements. This feature, enhanced Multiple Input Multiple Output (MIMO) [2] [3] transmission, uses the Reference Signals (RS) that guarantee efficient receiving of data information. MIMO systems, which are deployed spatial multiplexing, have emerged as one of the most promising approaches for high data rate wireless systems. Now MIMO is the main difference between LTE and LTE advanced uplink. This technique which is applied on the uplink of LTE advanced makes user equipment (UE) able to send up to four multiple unique parts of data in the same radio channel, instead of one sent in LTE uplink transmission. LTE supports a maximum of one spatial layer per UE (1×2, assuming an eNodeB diversity receiver) whereas LTE-advanced (release 10) supports up to four spatial layers of transmission allowing the possibility of 4×4 transmissions in the uplink, when combined with four evolved NodeB (eNodeB) receiver antennas [2] [6].

In this paper we will discuss the performance of the (2×2) MIMO LTE advanced system using different combinations of channel estimation and signal detection.

The paper is structured as follows. In Section 2, the LTE advanced system, which consists of transmitter and receiver, is described. A description of a flat Rayleigh channel model for (2×2) MIMO system is presented in Section 3. Section 4 introduces the demodulation reference signals used for channel estimation. Section 5 provides an outline of channel estimation and signal detection algorithms. Section 6 shows performance results in terms of simulated coded bit error ratio (BER) and coded throughput over different combinations of channel estimation and signal detection. Finally, Section 7 concludes the paper.

2. LTE Advanced System Model

In this chapter, we describe the LTE advanced uplink communication system [4]. Moreover, the differences between LTE and LTE advanced system are mentioned. The structure of the transmitter is also presented depending on the 3GPP LTE advanced standard [1].

2.1. Transmitter

In the transmitter, appropriate information bits are generated and Cyclic Redundancy Check (CRC) bits are calculated and added. Then the output is segmented to the code blocks and followed by 1/3 rate turbo coder. After that, the sequences are adapted by a rate matching process for a final suitable code rate. Moreover, the output of the rate matching is multiplexed and interleaved to get one stream of information data called codeword. All previous operations also happen in the LTE transmitter, but the LTE advanced transmitter can generate up to two different streams (codewords). This evaluation provides best in class performance attributes such as peak data rates and corresponding spectral efficiencies, capacity, and quality of service management. On the other hand, it is the cause of overall network complexity.

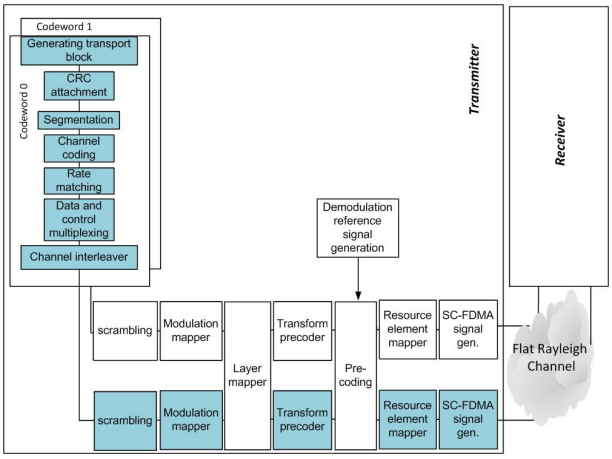

Fig. 1: LTE advanced system model.

There are two main differences between the two LTE releases 10 and 8 [1] [5], which are shown in Fig. 1. These main differences can be summarized in two additional blocks; layer mapper and precoding. The physical uplink shared channel (PUSCH) for LTE is represented with blue blocks. The LTE advanced transmitter contains both the white and blue blocks from the schematics.

In the case of LTE advanced, up to two different streams (codewords) can be mapped into a number of layers, depending on the configuration of the layer mapper block. The layer mapper divides the complex-valued modulation symbols into one or several transmission layers (up to four layers). The second difference is a pre-coding block which is responsible for more efficient transmission and provides higher link capacity and throughput.

To retrieve the transmitted signal in the receiver, the transmitter inserts occasional reference symbols into the data stream, which have a pre-defined amplitude and phase. This operation happens in resource elements mapper block after generating and pre-coding the reference signal.

Single Carrier Frequency Division Multiple Access (SC-FDMA) [6] is the best solution for the LTE advanced uplink due to the importance of low cubic metric and corresponding high power-amplifier efficiency. These are very important properties for user equipment because of the battery constraint on it as well as demanding construction of sufficiently linear power amplifiers.

In our simulation the transmitter consists of two codewords, two layers and two transmitter ports.

2.2. Receiver

After reception of the signal corrupted by the wireless channel, the uplink receiver aims to minimize the undesirable effects caused by mobile communication environment, using different channel estimation techniques [7].

The signal is received and processed at the receiver with inverse order of blocks, comparing with the transmitter. The LTE advanced uplink receiver is designed with channel estimation and signal detection. Then the signal is decoded and CRC is calculated. If the signal is received correctly, the receiver sends an acknowledgment to the transmitter and calculates the available bit error rate and throughput.

In the receiver, a channel estimation function measures the reference symbols, compares them with the corresponding transmitted ones and estimates the phase shift that the air interface introduced. The receiver then removes this phase shift from the information symbols, and recovers the information bits.

3. Radio Channel

Radio channel is a part of the communication link between the transmitter and the receiver and carries information in the form of electromagnetic waves. The radio channel is commonly characterized by scattering, attenuation, reflection, refraction and fading [8]. Studying radio channels helps us make an imagination about rapid fluctuations of radio signal amplitude over a period of time. The channel output y can be, in general, expressed by the convolution of a time-domain transmitted signal x with the channel impulse response h. The additive noise component n is also assumed to be present [6]:

$$y = h * x + n. \tag{1}$$

For the simplicity, this publication adopts a Flat Rayleigh channel model to describe the performance of the LTE advanced system. The Flat Rayleigh fading channel is the simplest Rayleigh channel which is used for narrowband transmissions over wireless and mobile communication channels. It is called flat because it has a constant attenuation factor during the subframe time and the whole allocated bandwidth. In our simulation, the attenuation factor is described as a constant complex number for every symbol in the subframe. In other words, the same complex number is applied on each resource element (RE) within a subframe.

For our LTE advanced system model with two transmitters and two receiver antennas, the transmitted signals are $(\mathbf{x_1}, \mathbf{x_2})$, received signals are $(\mathbf{y_1}, \mathbf{y_2})$, AWGN noise signals are $(\mathbf{n_1}, \mathbf{n_2})$ with the variance σ_w and the MIMO channel matrix has the following elements $(h_{11}, h_{12}, h_{21}, h_{22})$ for any discrete time sample. After taking these parameters into consideration we can model the MIMO channel using the simple matrix equation:

$$\begin{bmatrix} \mathbf{y_1} \\ \mathbf{y_2} \end{bmatrix} = \begin{bmatrix} h_{11} h_{12} \\ h_{21} h_{22} \end{bmatrix} \begin{bmatrix} \mathbf{x_1} \\ \mathbf{x_2} \end{bmatrix} + \begin{bmatrix} \mathbf{n_1} \\ \mathbf{n_2} \end{bmatrix}. \tag{2}$$

$$\Rightarrow \begin{array}{l} \mathbf{y_1} = h_{11}\mathbf{x_1} + h_{12}\mathbf{x_2} + \mathbf{n_1} \\ \mathbf{y_2} = h_{21}\mathbf{x_1} + h_{22}\mathbf{x_2} + \mathbf{n_2} \end{array}, \tag{3}$$

where

$$\begin{array}{l} \mathbf{x_1} = \{x_1(0), x_1(1), x_1(2), \ldots, x_1(k-1)\} \\ \mathbf{x_2} = \{x_2(0), x_2(1), x_2(2), \ldots, x_2(k-1)\} \end{array}, \tag{4}$$

and k is the length of the observed signal. Figure 2 describes the channel model used in our simulation.

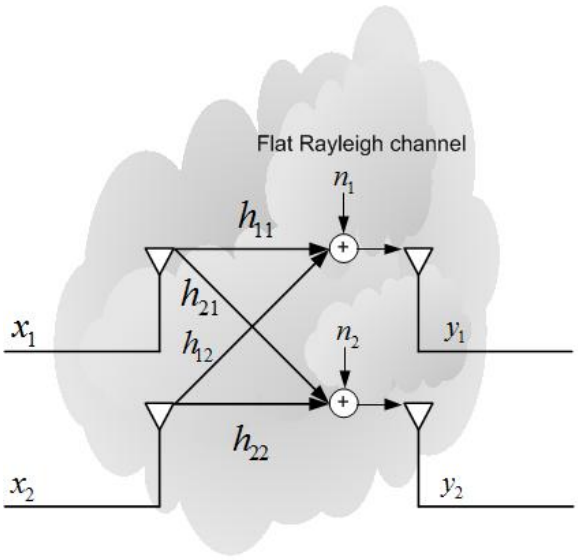

Fig. 2: Antenna and channel configurations for (2×2) MIMO systems.

4. Reference Signals

In this section, the basic structure of the uplink demodulation reference signal (DMRS) [1] [5] is described. DMRS is the most important component of channel estimation for efficient data reception. The LTE radio frame is 10 ms long and consists of 10 subframes of length 1 ms, each subframe contains 14 symbols as shown in Fig. 3. The exact position of the physical uplink shared channel DMRS (PUSCH DMRS) symbols in each uplink slot depends whether a normal or extended cyclic prefix (CP) is used [1]. In the case of uplink, the PUSCH demodulation reference signal is located in the fourth and eleventh symbols of each uplink subframe if this channel has a normal cyclic prefix and in the third and tenth symbols in the case of extended cyclic prefix [4]. In our case, we deal with normal cyclic prefix (14 symbols into a subframe).

4.1. Reference Signals for LTE

To support a large number of user equipment, a huge number of reference signal sequences $r_{u,v}^{(\alpha)}(n)$ [5] are generated. These sequences are defined by a cyclic shift α and a base sequence $\overline{r}_{u,v}(n)$ according to the Eq. (5).

$$r_{u,v}^{(\alpha)}(n) = e^{j\alpha n}\overline{r}_{u,v},\ 0 \leq n < M_{sc}^{RS}, \tag{5}$$

where: $u \in \{0, 1, \ldots, 29\}$ is the group number; v is the base sequence number within the group; M_{sc}^{RS} is the number of subcarriers in the reference signal. The cyclic shift α in the slot n_s is given as $\alpha = 2\pi n_{cs}/12$; n_{cs} is defined by Eq. (6).

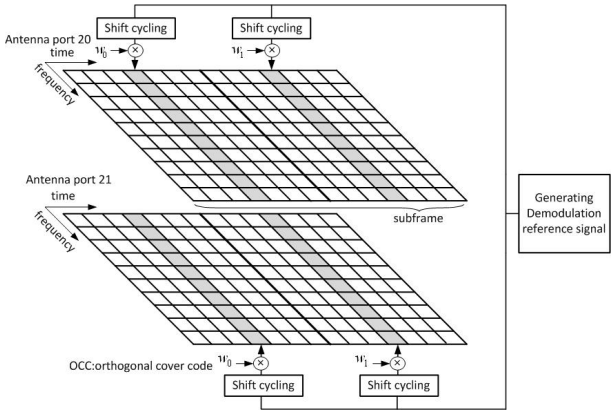

Fig. 3: Design of pilot pattern in a (2×2) MIMO SC-OFDM.

$$n_{cs} = \left(n_{\mathrm{DMRS}}^{(1)} + n_{\mathrm{DMRS}}^{(2)} + n_{\mathrm{PRS}}(n_s)\right) \mathrm{mod} 12, \tag{6}$$

where the value of DMRS parameters $\left(n_{\mathrm{DMRS}}^{(1)}, n_{\mathrm{DMRS}}^{(2)}\right)$ are given according to the table 5.5.2.1.1-2 in [5] and related to the cyclic shift

parameter provided by a higher layer. $n_{\mathrm{PRS}}(n_s)$ is calculated by the Eq. (7) [5], where $N_{\mathrm{symb}}^{\mathrm{UL}}$ is the number of SC-FDMA symbols in an uplink slot; $c(i)$ is a pseudo-random sequence.

$$n_{\mathrm{PRS}}(n_s) = \sum_{i=0}^{7} c\left(8N_{\mathrm{symb}}^{\mathrm{UL}} n_s + i\right) \cdot 2^i. \quad (7)$$

The demodulation reference signal sequence in LTE system $r^{\mathrm{PUSCH}}\left(mM_{sc}^{RS} + n\right)$ for PUSCH is defined by the Eq. (8) [5]. $m = 1, 2$ is a slot number in the subframe.

$$r^{\mathrm{PUSCH}}\left(mM_{sc}^{RS} + n\right) = r_{u,v}^{(\alpha)}(n). \quad (8)$$

4.2. Reference Signals for LTE Advanced

All previous DMRS equations consider only user equipment (UE) with a single transmit antenna. In LTE advanced multiple transmit antennas are used, so DRMS should be enhanced to meet new requirements. The solution for this development is generating multiple orthogonal reference signals using different phase rotations cyclic shifts (CSs). To provide mechanisms of orthogonally multiple DMRS transmission in MIMO spatial multiplexing schemes, LTE advanced defines DMRSs $r_{\mathrm{PUSCH}}^{(\lambda)}(.)$ associated with layer $\lambda \in \{1, 2, 3, 4\}$ [1]:

$$r_{\mathrm{PUSCH}}^{(\lambda)}\left(mM_{sc}^{RS} + n\right) = \boldsymbol{\omega}^{(\lambda)}(m) r_{u,v}^{(\alpha_\lambda)}(n). \quad (9)$$

The whole process of two layers demodulation reference signals generation depicts the Fig. 3. If we compare between the Eq. (5) and Eq. (9), we can distinguish two main differences between DMRS in the LTE and the LTE advanced. The first one is the orthogonal sequence $\boldsymbol{\omega}^{(\lambda)}(m)$ given in the table 5.5.2.1.1-1 [1] which separates the generated DRMS signal in two slots of one subframe. The second one is $n_{cs,\lambda}$ generated by the Eq. (10) [1].

$$n_{cs,\lambda} = \left(n_{\mathrm{DMRS}}^{(1)} + n_{\mathrm{DMRS},\lambda}^{(2)} + n_{\mathrm{PN}}(n_s)\right) \mathrm{mod} 12. \quad (10)$$

The main difference between the Eq. (6) and Eq. (10) is $n_{\mathrm{DMRS},\lambda}^{(2)}$ parameter which changes its value between layers to generate multiple orthogonal reference signals using different phase rotations (cyclic shifts). This means that Cyclic Shifts (CSs) of the DMRS base sequence are used to generate the DMRSs for the different layers. In addition to CSs as we mention, orthogonal cover codes (OCC) is used to get two different reference signals with in a subframe.

5. Channel Estimation and Signal Detection

Channel estimation is one of the fundamental issues which should be taken into consideration for LTE advanced system design. Channel estimation and signal detection are essential solutions to recover the transmitted signal with minimum interference. Channel estimation uses superimposed training sequences or pilot symbols to calculate the channel matrix. There are different techniques of channel estimation; two of them will be presented later.

As previously described, the pilot symbols are inserted periodically over the whole bandwidth. Therefore, block type pilot based channel estimation is an appropriate estimation method for the physical uplink signal in the LTE advanced system.

In this section, we present two typical approaches of channel estimation that can be used for block type pilots [7], known as least square (LS) and minimum mean-square error (MMSE) [9] [10].

Least square (LS) channel estimation is the simplest technique of channel estimation characterized by low complexity. It estimates the channel response by computing the division between received and transmitted symbols. The drawback of this approach is that the estimated symbols suffer from a high mean square error. This algorithm minimizes $||\mathbf{X}\mathbf{H}_{est} - \mathbf{Y}||^2$ which describes the distance between the received signal before and after the estimation. $\mathbf{Y}$ is a frequency-domain received pilot signal; $\mathbf{X}$ is a frequency-domain transmitted pilot signal; $\mathbf{H}_{est}$ is a frequency-domain estimated channel matrix. The LS channel estimation algorithm is based on Eq. (11) [10]:

$$\mathbf{H}_{est} = \mathbf{H}_{LS} = \left(\mathbf{X}^H\mathbf{X}\right)^{-1}\mathbf{X}^H\mathbf{Y}, \quad (11)$$

where $()^H$ denotes the hermitian transposition.

The minimum mean square error (MMSE) estimator gives better results than the LS estimator regarding mean square error. This estimation is based on the block type pilot arrangement. The major disadvantage of the MMSE estimation is its high complexity, which grows exponentially with a number of observations. This algorithm minimizes $E\{||\mathbf{H} - \mathbf{H}_{est}||^2\}$ which describes the distance between the received signal before and after the estimation. $\mathbf{H}$ is a channel matrix in frequency-domain. The MMSE channel estimation algorithm is based on the Eq. (12) [10].

$$\mathbf{H}_{est} = \mathbf{H}_{MMSE} = \mathbf{R}_{h,h_p}\left(\mathbf{R}_{h_p,h_p} + \sigma_w^2\mathbf{I}\right)^{-1}\mathbf{H}_{LS}, \quad (12)$$

where $\mathbf{R}_{h_p,h_p}$ is the autocorrelation matrix of the channel at the pilot symbol positions; $\mathbf{R}_{h,h_p}$ is the cross correlation matrix between the channel at the data symbol positions and the channel at the pilot symbol position

and $\mathbf{I}$ is the identity matrix. Now for the case of the block-type pilot channel estimation $\mathbf{R}_{h_p,h_p} = \mathbf{R}_{h,h_p}$.

Equation (12) can be modified as:

$$\mathbf{H}_{est} = \mathbf{H}_{MMSE} = \mathbf{R}_{h_p,h_p}\left(\mathbf{R}_{h_p,h_p} + \sigma_w^2\mathbf{I}\right)^{-1}\mathbf{H}_{LS}. \quad (13)$$

After estimating and calculating the channel matrix, the transmitted signal should be recovered from the received one. There are many signal detection techniques. In this publication, a zero forcing (ZF) and soft sphere detections are mentioned.

Zero-forcing (ZF) detection is the simplest signal detection technique. The detection matrix $\mathbf{G}$ is given by the pseudo-inverse of $\mathbf{H}_{est}$. The disadvantage of this technique is unconsidered correlation between the transmitter (user equipment) and the receiver (eNodeB), which leads to the highest error calculation. The ZF method cannot totally remove the inter-stream interference. It is less complex compared to the other techniques. More information about the ZF can be found in [11].

Soft Sphere detection (SSD): The main goal behind the SSD algorithm is to reduce the number of candidate symbol vectors during the codeword search. It is more complex than the ZF, but it gives better performance results. More information about SSD can be found in [12].

6. Simulation and Results

All the results were obtained by modifying the LTE uplink link level simulator developed at the Institute of Communications and Radio Frequency Engineering (INTHFT), Vienna University of Technology [13].

The LTE uplink link level simulator is one layer simulator. The structure of its transmitter corresponds to the blue blocks in the Fig. 1. The transmitter generates the data for given channel quality indicators (CQIs) [14], Signal to Noise Ratio (SNR) and number of subframes. In our case, thousand data subframes were generated to get more accurate simulation results. The CQI value gives us two kinds of information which are related to modulation order (4QAM, 16QAM, or 64QAM) and Effective Code Rate (ECR). These data are transmitted over the radio channel model. In the receiver, the channel estimation and signal detection take place to retrieve the original transmitted signal. Then the signal is decoded to generate an acknowledgment (ACK/NACKs) that is sent back to the transmitter. In LTE original uplink link level simulator [13], perfect channel knowledge is exploited and zeros are used instead of reference signals.

The modified version has the same basic structure of LTE uplink link level simulation. Some modifications are made to support new features of LTE advanced. These modifications can be clearly described in both transmitter and receiver. In the transmitter, two codewords instead of one are generated. Then two additional stages (layer mapper and pre-coding) are implemented to deal with two streams and two layers and provide more efficient receiving of the signal. After that we also generate demodulation reference signals for LTE advanced which are described in Section 4. All features of DMRS signal are taken into consideration. In the receiver, the reverse functions of the transmitter stages take place. Some modifications are done to fit a modified version of the transmitter. Moreover, estimation and detection techniques are modified to allow the application of (2×2) MIMO. This modification can be summarized in received signal filtering for both antennas to extract two transmitted signals, separately.

The simulation results are described as a relation between Bit Error Rate (BER) and Signal to Noise Ratio (SNR). Furthermore, LTE advanced uplink performance in terms of UE throughput is presented. In our simulation two estimators (LS and MMSE) and detection schemes (ZF and SSD) are employed. Different combinations of channel estimation and signal detection techniques are applied to compare between the performance of (2×2) MIMO and single input single output (SISO) systems.

In order to verify the performance of the LTE advanced system, we used different channel quality indicators (CQIs). For more details, we summarized the simulation parameters in the Tab. 1.

Tab. 1: Simulation parameters.

Parameters	Values
Bandwidth	1,4 MHz
FFT size (N)	128
Number of data subcarriers(Ntot)	72
CP length	'normal' [1]
Subcarrier spacing	15 kHz
Transmission setting	2×2
Channel model	Flat Rayleigh
Channel estimator	LS, MMSE
Detector	ZF, SSD
Channel quality indicator	6, 9, 15
Modulation schemes	4QAM 16QAM 64QAM

The results of simulations obtained with the modified LTE simulator supporting the LTE advanced features with the parameters setup according to Tab. 1 are shown in the Fig. 4 to Fig. 9. All the figures show that the best results are achieved when we used the MMSE and SSD combination, but it makes the system more complex. For lower complexity but suboptimal results, the LS and ZF combination can be used.

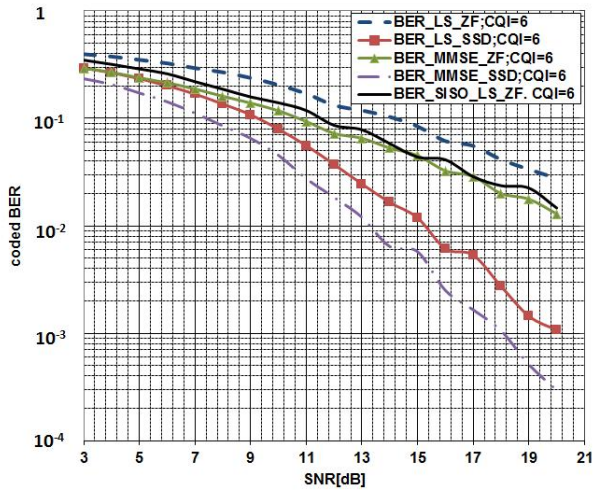

Fig. 4: Bit Error Ratio using 4QAM modulation for different combinations of the estimator and detector.

Figure 4, Fig. 5 and Fig. 6 show BER results for different CQI values. Seen from the point of view of used modulations, the figures describe the bit error rate for different modulation schemes (4QAM, 16QAM and 64QAM) respectively. In the three figures the black curve shows the LTE (SISO) uplink performance using a combination of least square (LS) and zero forcing techniques (ZF) [13]. The other curves give us an insight on the performance of the LTE advanced system with various combination of channel estimation and signal detection techniques.

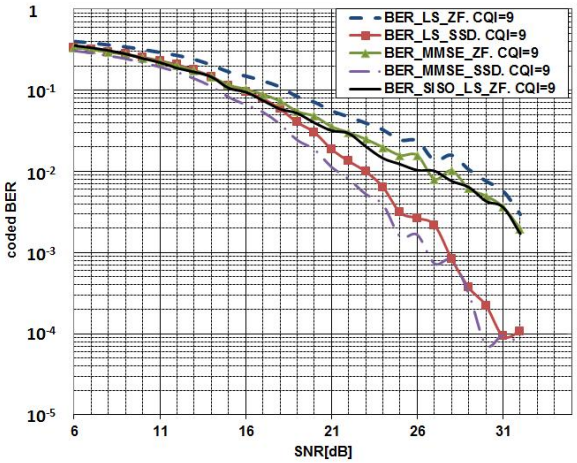

Fig. 5: Bit Error Ratio using 16QAM modulation for different combinations of the estimator and detector.

In terms of BER, the MMSE estimator slightly overcomes the performance of the LS estimator for all three CQI values and both signal detectors. For example of target $BER = 2 \cdot 10^{-2}$ the required SNR differs by approximately 3–4 dB for $CQI = 6$ and by 1–2 dB for $CQI = 9$ and 15. The use of SSD instead of the ZF detector results in the relaxing of SNR requirements for given fixed BER for both considered estimators. For the same target $BER = 2 \cdot 10^{-2}$ the system with SSD requires 6 dB lower SNR for $CQI = 6$, 5 dB lower SNR for $CQI = 9$ and 4 dB lower SNR for $CQI = 15$ than the system using the ZF detector.

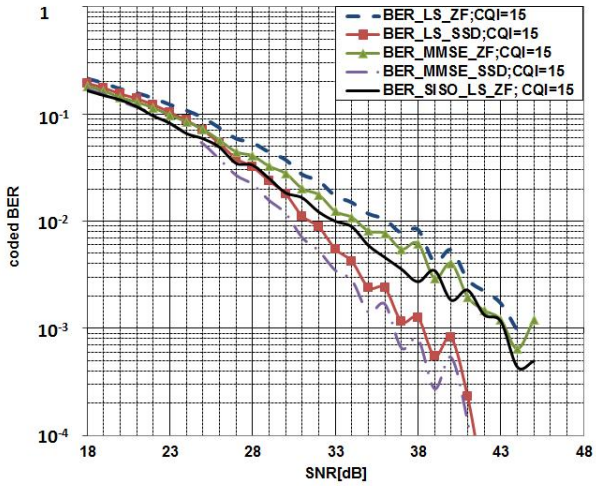

Fig. 6: Bit Error Ratio using 64QAM modulation for different combinations of the estimator and detector.

These curves also compare (2×2) MIMO transmission with a single input single output SISO one [13]. To evaluate the (2×2) MIMO transmission we present four combinations of channel estimation and signal detection. To achieve approximately the same bit error rate using a combination of LS and ZF in SISO transmission, MMSE and ZF combination should be applied during (2×2) MIMO transmission. The bit error rate for (2×2) MIMO transmission can be improved using more complex combinations (LS_SSD and MMSE_SSD) which were introduced in Section 5.

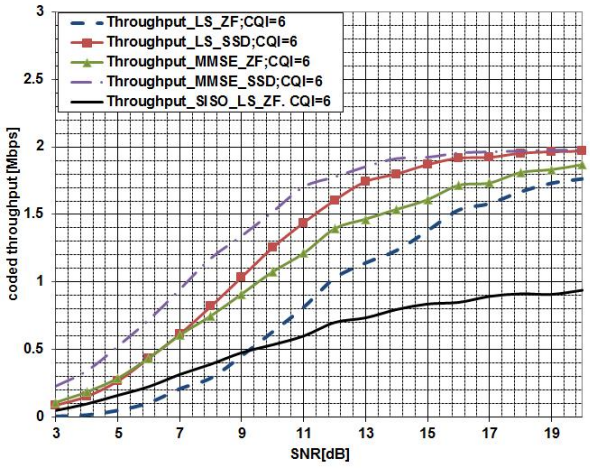

Fig. 7: Throughput curves using 4QAM modulation for different combinations of the estimator and detector.

Figure 7, Fig. 8 and Fig. 9 present the throughput performance results as a function of SNR for different CQI values. As for the BER case, the black curves depict the LTE uplink throughput using a combination of least square and zero force techniques [13]. The other curves show the throughput of LTE advanced system with various combinations of channel estimation and signal detection techniques. Apparently the achievable throughput increases with SNR.

The throughput performance for the $CQI = 6$ is illustrated in Fig. 7. In the case of 4QAM modulation (i.e. the $CQI = 6$), and the combination of LS and ZF method, the value of throughput for MIMO enabled overcomes the case of SISO for the SNR higher than 9 dB. Other combinations of channel estimation and signal detection with MIMO transmission give us higher throughput performance than SISO with ZF and LS even for SNR equal to 3 dB. Above 18 dB of SNR the LTE advanced performance is approximately doubled comparing with the LTE throughput.

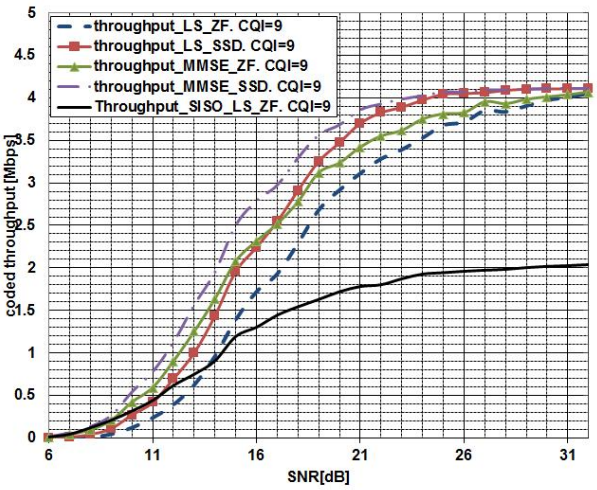

Fig. 8: Throughput curves using 16QAM modulation for different combinations of the estimator and detector.

Figure 8 compares the LTE and LTE advanced throughput performance for $CQI = 9$. The maximum value of 4 Mbps for the SNR above 26 dB can be achieved in this case. In the case of using the simple LS and ZF combination, the MIMO system should be enabled for the SNR above 14 dB in order to be beneficial.

The last results for the $CQI = 15$ and thus the 64QAM modulation are present in Figure 9. The MMSE estimator shows slightly better performance than LS estimator especially for lower SNR conditions (below 24 dB). This SNR value also delimits the usefulness of the (2×2) MIMO modes in comparison with the SISO system.

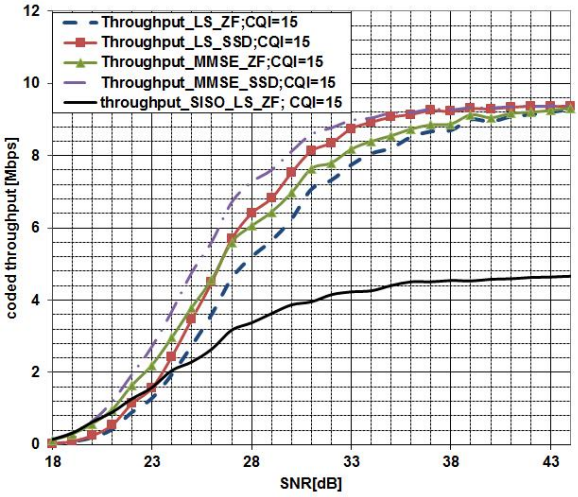

Fig. 9: Throughput curves using 64QAM modulation for a different combination of the estimator and detector.

7. Conclusion

This article gives a brief overview and description of the concepts of the LTE advanced system, its structure and the performance achievable using its MIMO configuration. In this paper we describe the extension of LTE Release 8 system by a (2×2) MIMO scenario of LTE advanced. We used a Flat Rayleigh channel model to simulate the performance of the system with different CQI configurations. Two channel estimation and signal detection techniques were presented. In order to perform the simulations, the LTE uplink link simulator was modified by implementing the basic LTE advanced MIMO features. The result shows the superior performance of the (2×2) MIMO LTE advanced system over the LTE with SISO configuration. The performance depends on the used channel estimation and signal detection techniques.

For future work, this research can be extended by evaluating the enhanced multi-antenna transmission technique performance in other channels like PedA, PedB, VehA and VehB. In addition, more complex MIMO scenarios, including multi-user arrangements can be considered.

Acknowledgment

This paper was supported by the internal project FEKT-S-11-12 MOBYS. The research has been performed in the laboratories of the SIX research center, reg. no. CZ.1.05/2.1.00/03.0072. The support of the project CZ.1.07/2.3.00/20.0007 WICOMT, the operational program Education for Competitiveness, is also gratefully acknowledged.

References

[1] 3GPP TS 36.211 Version 10.7.0. *Technical specification group radio access network; Physical Channels and Modulation*. In: *3GPP: 3rd Generation Partnership Project* [online]. 2013. Available at: http://www.3gpp.org/ftp/Specs/htmlinfo/36211.htm.

[2] SAWAHASHI, M., Y. KISHIYAMA, H. TAOKA, M. TANNO and T. NAKAMURA. Broadband Radio Access: LTE and LTE-Advanced. In: *International Symposium on Intelligent Signal Processing and Communication Systems, 2009. ISPACS 2009*. Kanazawa: IEEE, 2009, pp. 224–227. ISBN 978-1-4244-5015-2. DOI: 10.1109/ISPACS.2009.5383862.

[3] 4G Mobile Broadband Evolution: 3GPP Release 10 and Beyond HSPA+, SAE/LTE and LTE-advanced. In: *4G Americas* [online]. 2012. Available at: http://www.4gamericas.org/documents/4G%20Americas_3GPP_Rel-10_Beyond_2.1.11%20.pdf.

[4] DAHLMAN, E., S. PARKVALL and J. SKOLD. *4G: LTE/LTE-advanced for mobile broadband*. Amsterdam: Academic Press, 2011. ISBN 978-0-12-385489-6.

[5] 3GPP TS 36.211 Version 8.9.0. *Technical specification group radio access network; Physical Channels and Modulation*. In: *3GPP: 3rd Generation Partnership Project* [online]. 2009. Available at: http://www.3gpp.org/ftp/Specs/htmlinfo/36211.htm.

[6] SESIA, S., I. TOUFIK and M. BAKER. *LTE–the UMTS long term evolution: from theory to practice*. 2nd ed. Hoboken: Wiley, 2011. ISBN 978-047-0660-256.

[7] NIRANJANE, V. B. and D. B. BHOYAR. Performance analysis of different channel estimation techniques. In: *International Conference on Recent Trends in Information Technology (ICRTIT), 2011*. Chennai, Tamil Nadu: IEEE, 2011, pp. 74–78. ISBN 978-1-4577-0588-5. DOI: 10.1109/ICRTIT.2011.5972481.

[8] TRANTER, William H. *Principles of communication systems simulation with wireless applications*. Upper Saddle River: Prentice Hall, 2003. ISBN 01-349-4790-8.

[9] KEWEN, L. and X. KE. Research of MMSE and LS channel estimation in OFDM systems. In: *2nd International Conference on Information Science and Engineering (ICISE), 2010*. Hangzhou: IEEE, 2010, pp. 2308–2311. ISBN 978-1-4244-7616-9. DOI: 10.1109/ICISE.2010.5688562.

[10] SIMKO, M., D. WU, C. MEHLFUHRER, J. EILERTZ and D. LIU. Implementation Aspects of Channel Estimation for 3GPP LTE Terminals. In: *11th European Wireless Conference 2011 - Sustainable Wireless Technologies (European Wireless)*. Vienna: IEEE, 2011, pp. 1–5. ISBN 978-3-8007-3343-9.

[11] KIM, J. G. and W. S. CHOI. Joint ZF and partial ML detection for uplink cellular base station cooperation. In: *International Conference on ICT Convergence (ICTC), 2011*. Seoul: IEEE, 2011, pp. 321–326. ISBN 978-1-4577-1267-8. DOI: 10.1109/ICTC.2011.6082606.

[12] FU, W., C. ZHAO, W. WEI and Q. KONG. Improved sphere decoding algorithm in TD-LTE system. In: *IEEE 3rd International Conference on Communication Software and Networks (ICCSN), 2011*. Xian: IEEE, 2011, pp. 514–517. ISBN 978-1-61284-485-5. DOI: 10.1109/ICCSN.2011.6013645.

[13] BLUMENSTEIN J., J. COLOM IKUNO, J. PROKOPEC and M. RUPP. Simulating the long term evolution uplink physical layer. In: *Proceedings ELMAR, 2011*. Zadar: IEEE, 2011, pp. 141–144. ISBN 978-1-61284-949-2.

[14] KHOSHNEVIS, A., S. YAMADA, Z. YIN and S. CHOUDHURY. *Resource allocation and encoding for channel quality indicator (CQI) and CQI collided with uplink acknowledgment/negative acknowledgment* [patent]. USA. US 0088533 A1, 12/902,109. Issued 7.5.2013.

About Authors

Edward KASEM received his Master degree in electrical engineering at the Tishreen University in Syria in 2010. At present, he is a Ph.D. student at the Department of Radio Electronics, Brno University of Technology. His research interests are mobile communication systems based on OFDM.

Roman MARSALEK graduated at the Brno University of Technology in 1999 and received the doctoral degree from Universite de Marne-LaVallee, Ecole Superieure d'Ingenieurs en Electronique et Electrotechnique de Paris de Paris, France in 2003. He is currently assistant professor at the Department of Radio Electronics, Brno University of Technology in the Czech Republic. His research interests are in wireless communications theory and applied digital signal processing.

Jiri BLUMENSTEIN received his Master degree in electrical engineering from the Brno University

of Technology in 2009. At present, he is a Ph.D. student at the Department of Radio Electronics, Brno University of Technology.